

Mineralogical and Geochemical Analyses of the Maastrichtian Ironstones in Share-Tsaragi Area, Northern Bida Basin, Nigeria: Implications for Origin of the Ironstones

Ojo, O.J.^{1*}, Bamidele, T.E.², Adepoju, S.A.², Awe, A.¹,
Ndukwe, O.S.¹ and Omoyajowo, B.T.¹

¹Department of Geology, Federal University, P.M.B. 373, Oye Ekiti, Nigeria.

²Department of Geology and Mineral Science, Kwara State University, P.M.B. 1530, Malete, Nigeria.

Corresponding E-mail: olusola.ojo@fuoye.edu.ng

Abstract

The ironstones in Share-Tsaragi area, occur as capping for the extensive ridge of the Upper Cretaceous sequence in northern part of the Bida Basin, Nigeria. Methods of study include logging, sampling of the ironstones, mineralogical (thin section and X-ray diffraction) and geochemical analyses. Field study shows that the ironstone occurs as capping for the sequence of conglomerate, sandstone, siltstone and claystone. Generally, the ironstones are poorly sorted, massive and sandy to clayey. Goethite and hematite are the main iron minerals identified in the analyzed samples, with values ranging from 18.91 to 50.85% and 1.57 to 47.56% respectively, while quartz with values ranging from 30.25 to 50% (with exception of SH7M having the least value of 1.88%) and kaolinite (6.55 to 21.0%) represents the detrital materials. Geochemical composition presents variable concentrations of major oxides, trace and rare earth elements. The Fe₂O₃ (26.01-77.62 %, average of 42.2 %) constitutes the dominant major oxide, followed by SiO₂ and Al₂O₃ with range of values from 9.95 to 46.63 % and 3.15 to 15.13 % respectively. Predominance of iron oxide minerals (goethite and hematite) and low concentration of CaO, MgO and MnO (<0.5 %) suggest that iron oxide minerals were diagenetically precipitated as cements and replacement of the kaolinite precursor. Generally, the geochemical and mineralogical compositions of the analyzed samples suggest influence of lateritization in the formation of the ironstones. A genetic model involving transportation of the weathered products such as amorphous iron oxy-hydroxides and quartz, deposition in a non-marine environment and subsequent diagenetic iron enrichment of the detrital precursors is suggested. An enrichment of the analyzed samples in oxides of Al, Si, Na and K support terrigenous sources.

Keywords: Goethite, Detrital, Precursor, Lateritization, Tsaragi.

Introduction

The iron-rich sedimentary rock is defined by Petráněk and Van Houten (1997) and Stow (2005) as those containing 15% Fe or more and they are commonly referred to as ironstones or iron formations. Sedimentary iron ores can broadly be considered as occurring in three major classes: ironstones, bog iron ores, and (banded) iron formations (Craig and Vaughan, 1981). The origins of ironstone deposits have been traced to continental erosion, submarine volcanic springs, or upwelling ocean currents. The behavior of iron and its mineral precipitation are strongly controlled by the chemistry of the surface or diagenetic environment (Tucker, 1981), and according to Maynard (1983) may precipitate as ferric oxide or hydrate (hematite, maghemite, goethite, lepidocrocite), as a ferrous-ferric oxide (magnetite), as a ferric-ferrous silicate (glauconite), as a ferrous-ferric silicate (greenalite, chamosite), as a carbonate (siderite), or as a sulfide (pyrite, marcasite, or less stable precursors).

The sedimentary ironstones in various part of the world have attracted the attention of different researchers. The

Phanerozoic sedimentary ironstones was described by Young and Taylor (1989) as thin beds deposited in a wide range shallow marine to non-marine environments. Loope *et al.* (2012), Afify *et al.* (2018) and Akinlotan (2019) provided more insight on the iron bearing sediments as related to their origin, diagenetic history and paleoenvironmental significance. Previous studies by Adeleye (1973) and Mücke *et al.* (1999) revealed the occurrence of ironstones in Batati (northern Bida Basin) and Agbaja (southern Bida Basin) areas respectively as a consistent and resistant cap of oolitic and pisolitic ironstones. Ladipo *et al.* (1994), Abimbola *et al.* (1999) and Mücke (2000) studied the facies analysis, petrography, mineral paragenesis and geochemical characteristics of Agbaja ironstone and concluded they were derived from a kaolinite precursor. Recently, Ojo *et al.* (2020) concluded that ironstones of the Patti Formation at Ahoko and Geheku areas (southern Bida Basin) occur as interbeds with argillaceous rocks in form of bands and lenses.

The investigated ironstone in this present study is located at Share-Tsaragi axis which is bounded by longitudes E004°54' - 005°00' and latitudes N008°45' -

009°00' in the northern part of Bida Bida Basin, northcentral Nigeria (Fig. 1). The scientific data on the ironstones unlike the widely reported oolitic and pisolitic ironstones in the Bida basin is lacking in spite of its lateral persistence and as extensive cap for the sedimentary sequence of underlying sandstones and claystones (Agbonna ridge). Recent studies on sedimentological characteristics of the sandstones in the northern Bida Basin include Ojo and Akande (2012) which concluded that the Bida Formation around Share-Patigi area is composed dominantly of siliciclastic sediments of fluvial processes that have undergone short transportation history and Adepoju *et al.* (2020) which reported that the siliciclastic sediments in the northern Bida basin which are dominated by quartzarenite to sublitharenite petrofacies and were

derived from plate interiors or stable continental areas and deposited in a stable intra-cratonic basin. In the present investigation the amorphous ironstones overly the siliciclastic sediments and laterally extensive along the east west depositional strike.

The aim of this present work is to determine the field characteristics, mineralogy and geochemical composition of the ironstones within which is presently unknown. The field characteristics, mineralogical and geochemical data obtained from the ironstone samples were used to develop a genetic model and compared it with other well known contemporary deposits around the world. This study is significant, because for the first time, information on the origin, processes and genetic significance of the ironstones is provided.

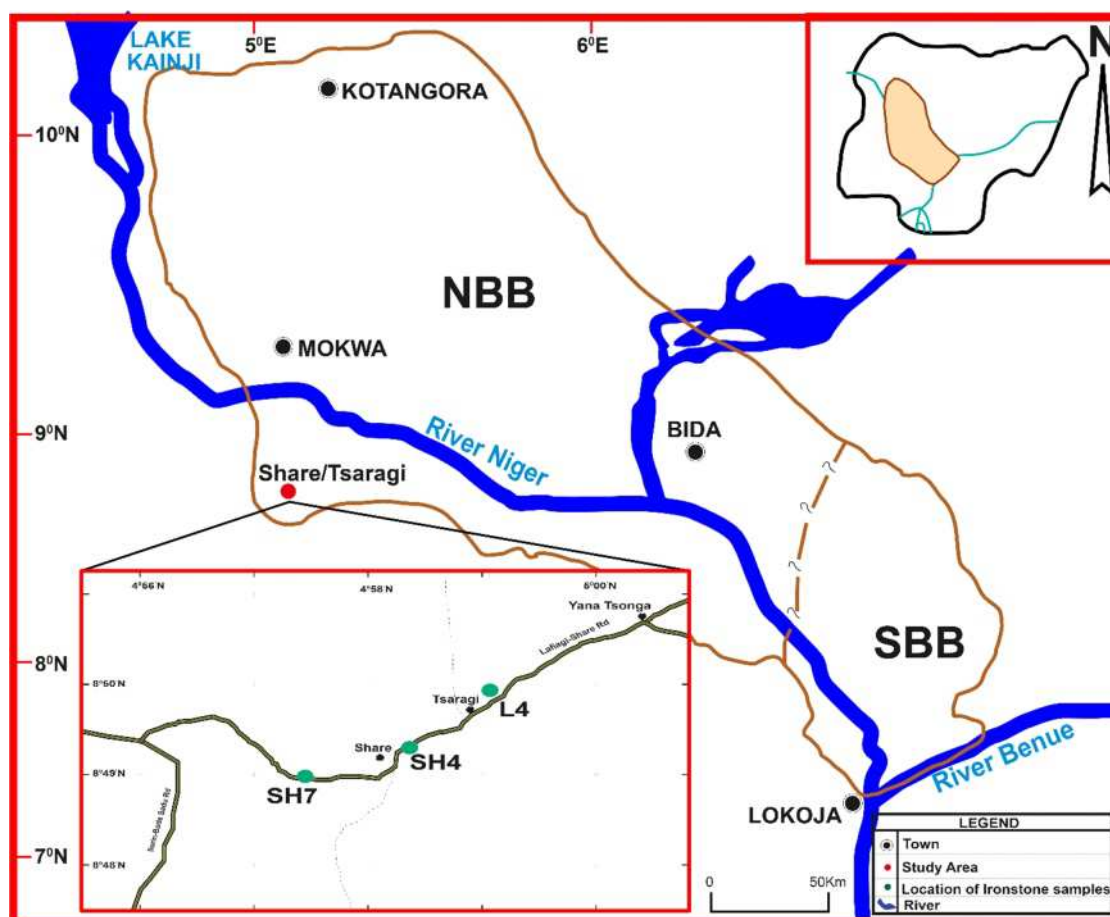


Fig. 1. Map of Nigeria (Inset) showing the position of Bida Basin and the location of the study area within the Bida Basin (After Adepoju *et al.* 2020). Note: NBB - Northern Bida Basin; SBB - Southern Bida Basin.

Geological and Stratigraphic Settings

A review of available earlier literature is indicative of rift related origin for the Bida Basin (King, 1950; Kennedy, 1965). Kogbe *et al.* (1983) and Ojo and

Ajakaiye (1989) advanced arguments supported with geophysical and satellite data, in favour of rift origin associated with drifting apart of South America and Africa plates. They agreed that Bida Basin is part of the tectonic evolution of the Benue Trough which began in

petrological procedure at the thin section workshop and microscope laboratory of the Department of Geology and Mineral Sciences, Kwara State University, Malete, Nigeria.

Mineralogical composition of five selected samples were also determined using x-ray diffraction (XRD) analysis carried out at the Department of Geology, Faculty of Natural and Agricultural Sciences, University of Pretoria, South Africa. Prior to analysis, selected samples were pulverized into finer materials using a riffle splitter and the samples were loaded in a tungsten carbide vessel and prepared according to the standardized Panalytical backloading system, which provides nearly random distribution of the particles. They were then analyzed using a PANalytical X'Pert Pro powder diffractometer in θ - θ configuration with an X'Celerator detector and variable divergence- and fixed receiving slits with Fe filtered Co-K α radiation ($\lambda = 1.789 \text{ \AA}$). The phases of minerals present with their distinctive peaks were identified using X'Pert Highscore plus software. The relative phase amounts (weight%) were estimated using the Rietveld method (Autoquan Program) based on the relative peak intensities of the respective minerals in the XRD charts.

Five samples (SH4K, SH4J, SH7L, SH7M and L-4T) were subjected to inorganic geochemical analysis to determine the bulk composition of major oxides, trace and rare earth elements using x-ray fluorescence (XRF) and inductively coupled plasma mass spectrometry (ICPMS) and these were carried out at the Acme Analytical Laboratories, Vancouver, BC, Canada. Prior to analysis, selected samples were split and pulverized via a jaw crusher to 70% passing a 10 mesh (2 mm), then further pulverized to 85% passing 200 mesh (75 μm) in a mild-steel ring-and-puck mill. A 0.20 g aliquot was weighed into a graphite crucible and mixed with 1.50 g of LiBO₂/Li₂B₄O₇ flux. The crucibles were later heated in a 980°C oven for 30 minutes and resulting bead was dissolved in 5% HNO₃ (ACS grade nitric acid diluted in demineralized water). Samples and calibration reagent blanks were aspirated into an XRF (SpectroCiros Vision or Varian 735) to determine the set of major oxides. Samples for ICPMS analysis were further pulverized to 95% passing 150 mesh (100 μm) in a mild-steel ring-and-puck mill. A 0.20 g aliquot was weighed into a graphite crucible and mixed with 1.50 g of LiBO₂/Li₂B₄O₇ flux. The crucibles were heated in a 980 °C oven for 30 minutes. The resulting bead was dissolved in 100 mL 5% HNO₃ (ACS grade nitric acid diluted in demineralized water). An aliquot of the solution was poured into a polypropylene test tube. The

samples and calibrated reagent blanks were aspirated into an ICPMS (PerkinElmer Elan 6000 or 9000) and a digested split of 0.5 g in Aqua Regia aspirated into an ICP-MS to determine the elemental compositions.

Results

Field Characteristics

The investigated ironstones at Share-Tsaragi area of the Bida Basin occur as a laterally continuous cap over the Campanian-Maastrichtian sedimentary pile and in association with conglomerate, sandstone and claystone in the study area (Figs. 3 and 4). At the western bound of the Agbona ridge, (N08°48'58" and E004°57'27"), the ironstone formed a thick cover of about 10 m on top of the generally fining upward sequence. Generally, the ironstones are massive, that is no organized internal structure, with varying thickness and laterally persistent (Figs. 4a and b). At the central part of the ridge (N08°49'18" and E004°58'21") and Tsaragi (eastern bound of the ridge, N8°41'28.9" and E004°58'24.6") along Share-Pategi highway, the ironstones, about 5.0 and 2.0 m thick respectively, overly interbeds of sandstone, and sandy claystone. The ironstone is brownish to yellowish in colour, poorly sorted, medium to coarse grained and in some cases, pebble sized detrital quartz clasts are common. The composition is essentially made up of sand and silt size detrital quartz grains cemented by iron oxide minerals.

The yellowish-brown to reddish and dark brown coloration of the ironstone is suggested to be an illustrative of varying level of iron enrichment from iron pigmentation to partial and total iron replacement. The colour variation is also suggested to be indicative that the iron minerals are largely precipitated as diagenetic replacement for the clay precursors.

Petrography and Mineralogy

Petrography of each thin sections was described using an optical microscope, to ascertain mineral variety and their texture. X-ray diffraction (XRD) was also carried out on samples to determine their mineralogical compositions. Thin section microscopy studies generally revealed framework composition, consisting essentially of angular, monocrystalline and poorly sorted quartz (Figs. 5a and b). The quartz floats within the hematitized clay matrix and in few cases exhibit point contacts. In most places, iron cement coatings were observed around the quartz grains.

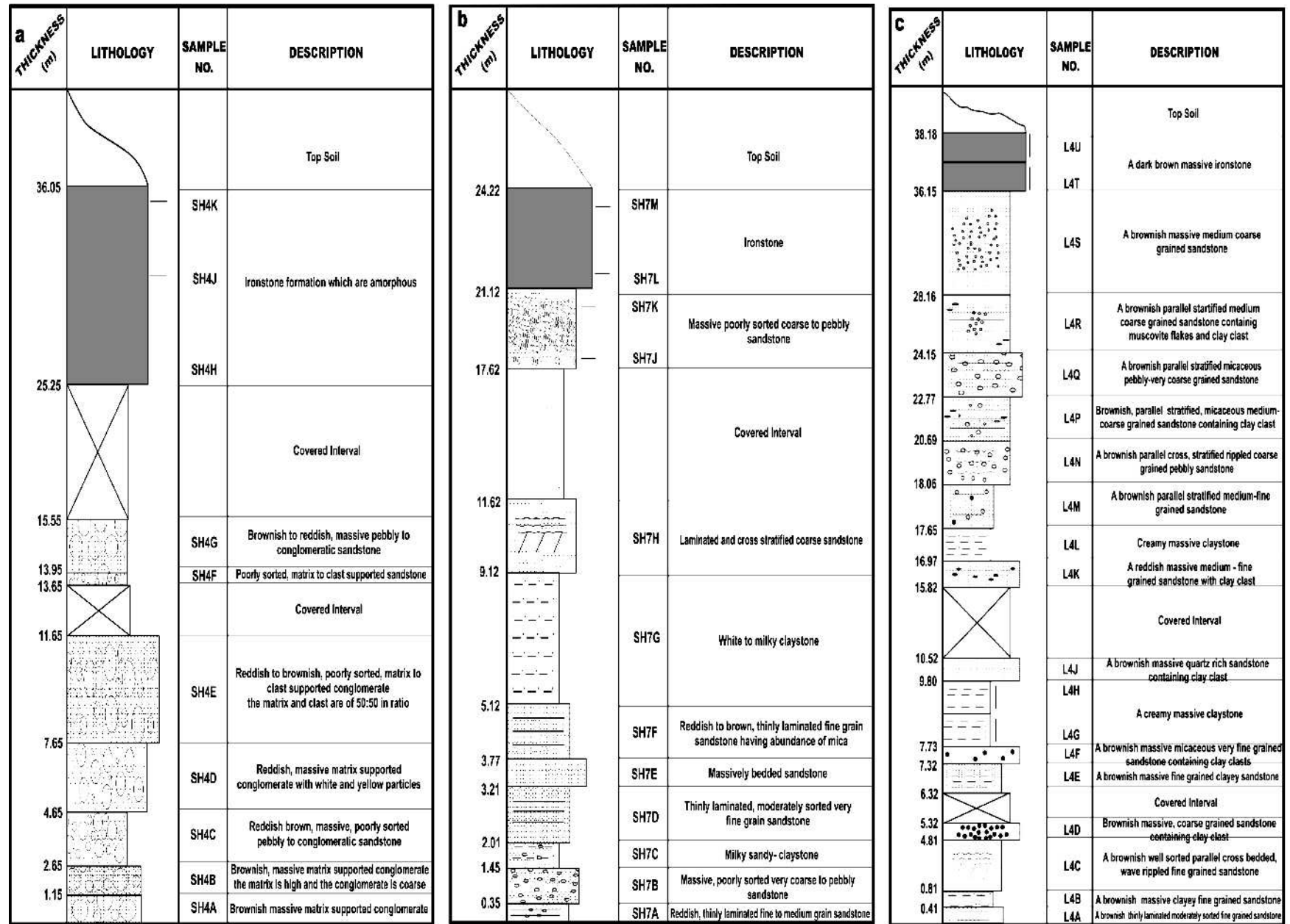


Fig. 3: Lithological section of Enagi Formation (a) at Agbona ridge near Agbona High school, Share (N08°48'58" and E004°57'27"); (b) Agbona ridge behind Share market east of Agbona high school (N08°49'18" and E004°58'21") and (c) at Tsaragi, eastern bound of Agbona ridge (N8°41'28.9" and E004°58'24.6").



Fig. 4: Field photograph showing (a) Ironstone bed IB at Agbona Ridge, Agbona high school, Share and (b) Ironstone bed IB at Tsaragi (Note the contact between the sandstone and the ironstone layer). The ironstone occurs as laterally consistent and resistant cap over the underlying sandstone and claystone. The man backing the exposure is about 1.7m tall.

The mineral species identified from the XRD diffractograms (Fig. 6a and b) include: quartz (SiO_2), hematite ($\alpha\text{-Fe}_2\text{O}_3$), with a minor amount of goethite ($\alpha\text{-FeOOH}$) and kaolinite [$\text{Al}_2(\text{SiO}_3)(\text{OH})$]. The relative abundance of the identified minerals as presented in table 1 and it reveals the iron minerals as goethite (18.91-50.85%) and hematite (1.57-47.56%). Other minerals present include quartz (30.25-50%) and kaolinite (6.55-21%). Among all the analyzed samples, SH7M show different mineralogical composition

compare to others with relatively low percentage of quartz (1.88%) but relatively high amount of goethite, hematite and kaolinite.

Geochemistry

The major, trace and rare-earth element (REE) compositions of the analyzed 5 samples from the 3 sections are hereby present in tables 2, 3 and 4. The oxides of Iron (Fe_2O_3) vary in contents between 26.01

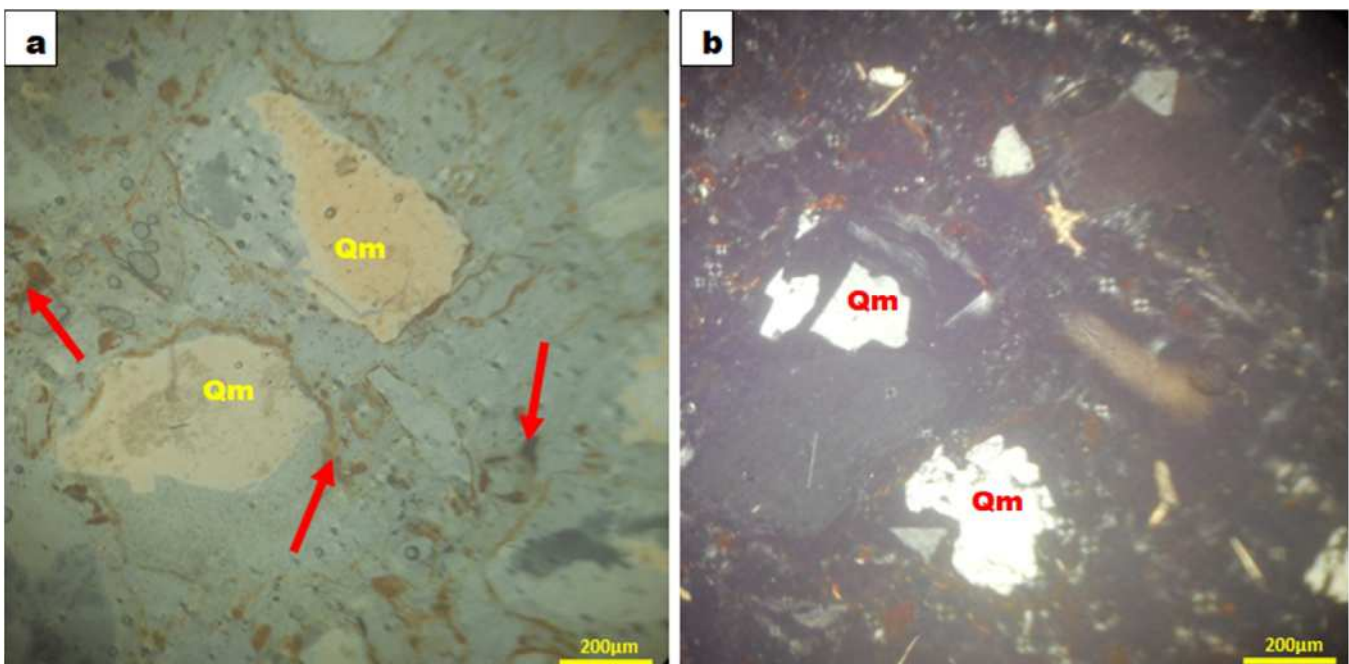


Fig. 5: Photomicrograph of ironstone sample L4T (a- PPL, b- XPL). Note the floating angular quartz grains (Qm) in the matrix of kaolinitic clay and iron oxide cement (arrow).

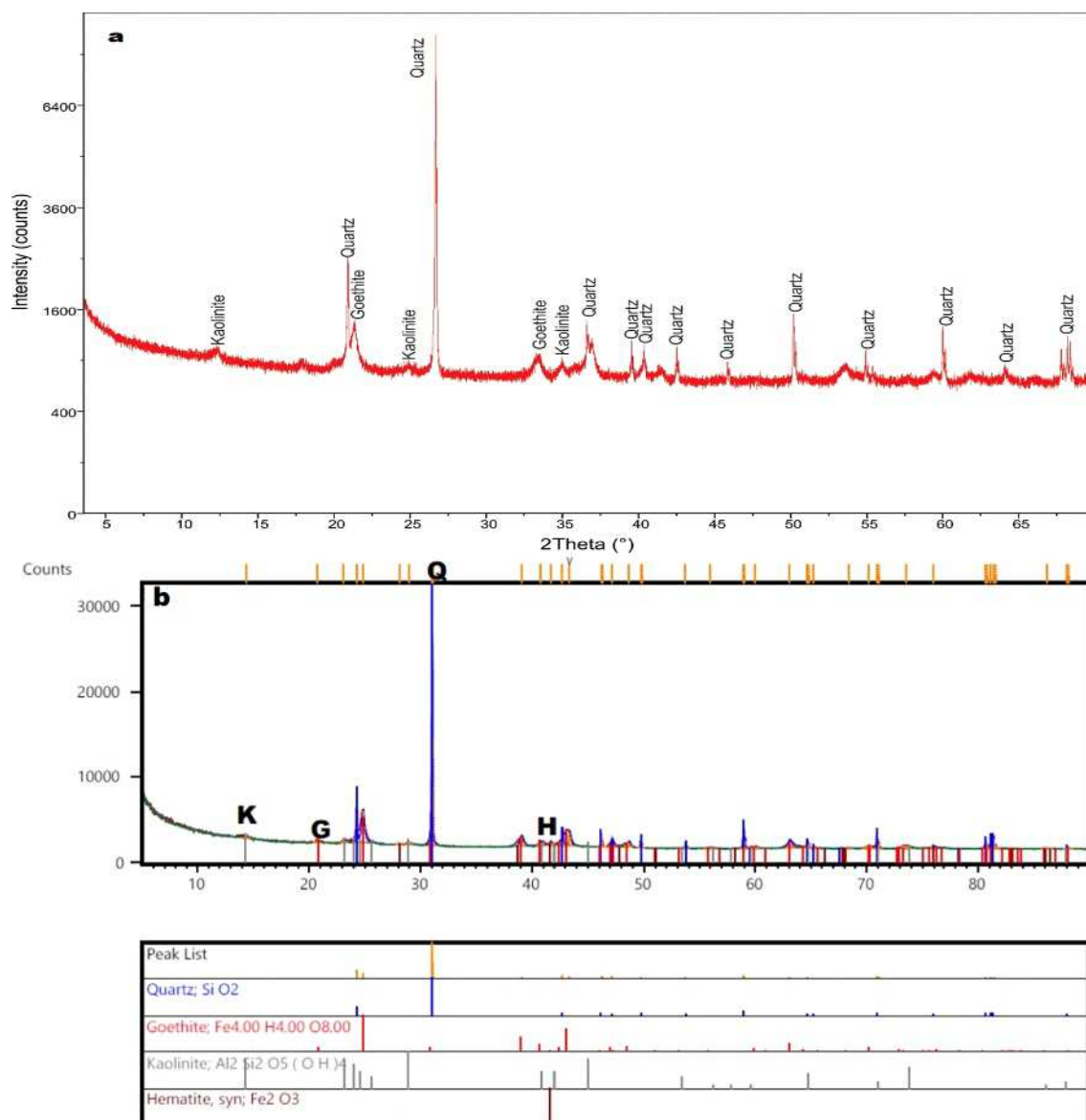


Fig. 6: X-Ray Diffraction result showing mineral peaks for (a) ironstone sample L4T and (b) ironstone sample SH4J. Note the mineral compositions; K-Kaolinite, G-Goethite, Q-Quartz and H-Hematite.

Table 1: Quantitative mineral composition (%) of the studied ironstones obtained from the XRD analysis

Sample Minerals	SH4K	SH4J	SH7L	SH7M	L-4T
Goethite	49.28	50.85	18.91	31.84	29.00
Hematite	2.92	1.57	25.10	47.56	ND
Quartz	37.49	30.25	49.44	1.88	50.00
Kaolinite	10.31	17.33	6.55	18.72	21.00

and 77.62%, alumina (Al_2O_3) contents between 3.15 and 15.13%, silica (SiO_2) contents vary between 9.95 and 46.63% while other oxides (CaO , MgO , K_2O and Na_2O) have concentrations less than 0.5%. The compositions reflect and support the presence of iron minerals

(goethite and hematite), quartz and kaolinite as mineral constituents in the ironstones.

There is a variation in the SiO_2 , Al_2O_3 and Fe_2O_3 contents; 4 samples (SH4H, SH4J, SH7L and L-4T) have relatively higher SiO_2 and Al_2O_3 contents compare to sample SH7M indicating low iron replacement whereas the sample SH7M with relatively lower SiO_2 and Al_2O_3 has higher Fe_2O_3 content which indicate more ferruginization. Iron enrichment in SH7M might also probably be due to preferential iron replacement influenced by relief because the sample was collected from the topographically high point of the ridge in the study area.

Trace elements concentrations (ppm) obtained in the studied ironstone and published data from other parts of Nigeria and Egypt are presented in table 3. The trace element compositions of the ironstone samples display an enrichment in Barium (Ba), Chromium (Cr) and Vanadium (V) with contents varying respectively from 19.00 to 618.10 ppm, 58.20 to 371.00 ppm and 171.00 to 421.00 ppm. They are however relatively low in transition metals and high field strength elements (Sc, V, Nb, U, Th, Zr, Hf, Pb), therefore, suggesting some contributions from felsic materials in the source region. Thus, the elemental variations above might suggest sediments source from detrital origin as the element depletion might be as a result of competing clastic and chemical sedimentation.

The ironstone possesses REE concentrations ranging from 30.22 to 286.66 ppm and enriched in light rare earth element (LREE) contents (27.19-280.10 ppm) but

depleted in the heavy rare earth elements (HREE) contents (2.81-17.83 ppm) values (Table 4). It is to be noted that positive Eu (0.96-1.24) and Ce (2.21-2.30) anomaly were recorded for all the studied samples which might indicate same process of iron formation. NASC normalized values La/Sm (0.55-1.06), La/Lu (0.56-1.88) and Tb/Lu (0.9-01.58). The REE concentrations of the ironstone were normalized using REE values of North American Shale Composite (NASC; Gromet *et al.*, 1984) and the displayed REE patterns of all the ironstones exhibits flat REE pattern, variable LREE depletions, a distinctly positive Ce anomaly with no Eu anomalies (Fig. 7). We observed that all the ironstones display REE patterns only very slightly depleted in LREE compared to the NASC (Fig. 7). The strong similarities and consistent of the REE patterns for all the ironstones suggest that these sediments gain their REE from detrital sources.

Table 2: Major Element (%) composition of the investigated ironstone samples obtained from geochemical analysis and those from some referenced deposits

Sample Code	N=5					Ranges of values			
	SH4H	SH4J	SH7L	SH7M	L-4T	Share-Tsaragi, Northern Bida Basin (Present Study)	Ironstone from Putti Formation, Southern Bida Basin (Ojo <i>et al.</i> , 2020)	Sideritic Ironstone from Leru, Anambra Basin (Akande and Mücke, 1993)	Ironstone from El Bahariya Depression, Western Desert, Egypt (Salama <i>et al.</i> , 2012)
SiO ₂	46.30	39.46	55.05	9.56	46.63	9.56-55.05	8.41-52.50	10.70-43.00	1.85-19.73
Al ₂ O ₃	15.13	10.49	3.15	4.98	9.27	3.15-15.13	1.79-7.49	3.69-7.84	1.02-5.62
Fe ₂ O ₃	26.01	37.72	35.94	77.62	33.79	26.01-77.62	36.46-49.72	10.77-17.90	68.86-89.45
CaO	0.08	0.02	0.01	0.02	0.07	0.01-0.08	0.08-13.97	3.91-4.54	0.06-2.73
K ₂ O	0.13	0.07	0.02	0.02	0.03	0.02-0.13	0.10-0.47	0.18-0.21	0.09-0.82
MgO	0.10	0.06	0.11	0.04	0.07	0.04-0.11	0.05-2.84	4.69-5.05	0.31-1.45
MnO	0.36	0.11	0.04	0.23	0.06	0.06-0.23	0.01-1.19	0.37-0.44	0.21-10.03
Na ₂ O	0.01	0.01	0.01	0.01	0.01	0.11	0.01-0.16	0.06-0.07	0.08-1.98
P ₂ O ₅	0.11	0.33	0.21	0.48	0.87	0.11-0.87	0.04-8.81	1.86-1.98	0.09-0.66
TiO ₂	0.88	0.68	0.36	0.23	0.73	0.23-0.88	0.29-0.88	0.22-0.34	0.00-0.24

Discussion

Diagenesis, Paleoenvironments and Genetic model

Review of previous studies on ferruginous sediments by Lepp and Goldich (1964), Cotter and Link (1994), Mücke (2000), Lottermoser and Ashley (2000) among others have proposed number of mechanism origin and genetic models for ironstone formation including sub-aerial weathering of pre-existing rocks, hydrothermal alteration, diagenesis, upwelling water and depositional. In this study, the textural, mineralogical and geochemical characteristics of the ironstones within Share-Tsaragi area in the northern Bida Basin suggest

diagenetic supergene enrichment origin. Petrographic studies reveal botryoidal texture with syneresis cracks as the main colloidal texture of the iron cement (Figs. 5a and b) and this is an indication of iron precipitation and replacement occurring as post-depositional (early diagenetic) to be the main processes that has modified the ironstone. The presence of quartz in the ironstones as indicated by the qualitative (Figs. 6a and b) and quantitative (Table 1) of the mineralogical compositions is indicative of detrital minerals derived from continental weathering of crystalline protoliths. The quartz is suggested to be one of the clastic components that were contributed from periodic influx of surface-transported materials, which were in part intermixed

Table 3: Trace elements (ppm) composition of the investigated ironstone samples obtained from geochemical analysis and those from some referenced deposits

Sample Code	N=5					Ranges of values of referenced deposits			
	SH4H	SH4J	SH7L	SH7M	L-4T	Share-Tsaragi, Northern Bida Basin (Present Study)	Ironstone from Patti Formation, Southern Bida Basin (Ojo et al., 2020)	Sideritic Ironstone from Leru, Anambra Basin (Akande and Mücke, 1993)	Ironstone from El Bahariya Depression, Western Desert, Egypt (Salama et al., 2012)
Ba	618.10	187.30	19.20	19.00	133.80	19.00-618.10	15.70-483.10	66.00-75.00	98.00-8982
V	305.00	421.00	171.00	193.00	377.00	171.00-421.00	21.40-93.00	459.00-530.00	64.40-1483
Cr	170.20	179.70	58.20	78.60	371.00	58.20-371.00	12.70-26.60	79.00-131.00	8.20-328.00
Pb	57.97	17.40	19.44	13.67	5.50	5.50-57.97	8.49-27.78	14.00-21.00	1.53-168.30
Cu	28.72	49.28	3.73	9.07	25.40	3.73-49.28	4.11-14.22	5.00	0.60-18.45
Zr	22.80	23.10	10.30	19.40	379.00	19.40-379.00	2.60-12.10	1.49-176.00	10.00-29.80
Zn	14.30	26.20	145.40	71.70	29.00	14.30-145.40	25.00-178.50	177.00-270.00	77.00-1986
Th	13.40	12.40	2.50	2.40	8.73	2.40-12.40	4.70-9.60	Not Reported	Not Reported
Co	10.10	8.70	9.60	17.80	12.50	23.50-17.80	0.80-50.50	15.00-84.00	0.43-87.60
Ni	7.50	9.80	11.50	23.50	16.80	7.50-23.50	2.80-23.90	13.00-24.00	3.80-263.60
Sr	6.20	3.20	9.40	4.00	75.00	3.20-75.00	6.00-1065.80	149.00-169.00	3.92-696.00
U	5.90	13.00	7.90	7.60	21.41	5.90-21.41	1.70-4.70	Not Reported	2.04-14.48
Mo	4.76	8.50	2.30	2.16	4.94	2.30-8.50	0.26-0.76	Not Reported	5.00-99.00
Rb	4.40	3.10	0.20	0.30	1.50	0.20-4.40	0.50-4.10	9.00	Not Reported
Nb	0.09	0.38	0.47	0.27	18.80	0.09-18.80	0.05-0.41	20.00-21.00	Not Reported

Table 4: Average Rare earth element (REE) concentrations of the Share-Tsaragi Ironstones compared with the Published values North Archean Australian Shale (NASC) after Gromet et al. (1984).

Sample Code	SH4J	SH7L	SH7M	SH4H	L-4T
La	9.50	6.00	6.70	14.10	43.40
Ce	34.30	13.50	14.80	245.30	80.90
Pr	3.36	1.43	1.74	3.97	9.97
Nd	12.11	5.25	6.73	14.10	38.30
Sm	3.13	1.01	1.56	2.63	7.54
Eu	0.62	0.22	0.35	0.55	1.50
Gd	2.32	0.62	1.72	1.95	6.63
Tb	0.35	0.15	0.30	0.32	0.86
Dy	2.19	0.86	1.77	1.65	4.46
Ho	0.38	0.16	0.40	0.33	0.78
Er	1.02	0.39	1.16	0.79	2.09
Tm	0.18	0.06	0.15	0.13	0.32
Yb	0.94	0.50	1.04	0.73	2.34
Lu	0.15	0.07	0.18	0.11	0.35
ΣREE	70.55	30.22	38.60	286.66	199.44
ΣLREE	62.40	27.19	31.53	280.10	180.11
ΣHREE	7.53	2.81	6.72	6.01	17.83
ΣLREE/ΣHREE	8.29	9.68	4.69	46.61	10.10
Eu/Eu*	1.03	1.24	0.96	1.08	0.94
Ce/Ce*	2.27	2.23	2.30	2.21	2.24
La _N	0.31	0.19	0.22	0.45	1.40
Ce _N	0.51	0.20	0.22	3.68	1.21
Nd _N	0.44	0.19	0.25	0.51	1.40
(La/Sm) _N	0.55	1.06	0.79	0.96	1.04
(La/Lu) _N	0.94	1.27	0.56	1.88	1.84
(Tb/Lu) _N	1.24	1.20	0.90	0.901.58	1.33

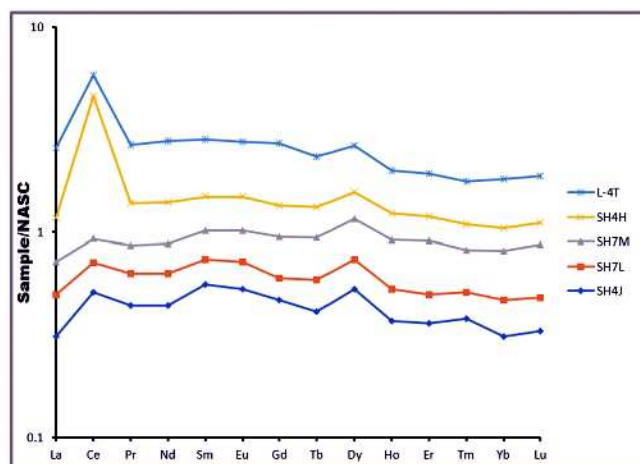


Fig. 7: Share-Tsaragi ironstone REE normalized plot to values of North Archean Australian Shale (NASC) after Gromet *et al.* (1984).

with the products of chemical precipitation during diagenesis. Also, the submission of Boyd and Scott (1999), sediments enrichment of sediments in Zn, Pb, Mo, V and As with depletion in Co, Ni and Cu characterizes deposits from hydrothermal precipitations, therefore, the studied ironstone with low concentrations of Zn, Ni, Pb, Zn and Sr cannot be attributed to hydrothermal source but rather diagenesis.

The major oxide content of iron (Fe_2O_3) with concentrations of Zr, Zn, V and Pb indicate elemental re-concentration in the sediment according to Lottermoser and Ashley (1996). Also, trace elements concentrations of some ferromagnesian elements (e.g. Cr, Ni, and V) are likely to have been sourced from basic rocks in adjacent areas of the basin Khan *et al.* (1996). The relatively low concentrations of Co (23.50-17.80 ppm), Ni (7.50-23.50 ppm) and Pb (5.50-57.97 ppm) may be attributed to terrigenous debris contributions on a continental margin. Also, high Cr content in the ironstone (58.20-371.00 ppm) is typical of material derived from mafic and intermediate rocks with the residual elements upon lateralization thereby confirming detrital origin of the ironstones. Binary plot of Na against Mg (after Nicholson, 1992) presented in Fig. 8 confirm freshwater origin for the ironstones while ternary plots of Si-Al-Fe and Si-Al-(Ca+Mg) presented in Figs. 9a and b respectively exhibit similarity with the Neoproterozoic ironstones in the eastern part of the Adelaide Geosyncline, South Australia (Lottermoser and Ashley, 2000) which are also from diagenetic origin. The iron minerals occur mainly as pore filling cement and they do not exhibit any close mineralogical and micromorphological resemblance with the two types of ferruginous deposits from Silurian of the Carnic Alps in Austria which Ferretti (2005) regarded as

microbial deposits due to their common biogenic origin. Other evidences that ruled out the possibility of organisms' involvement in the formation of the ironstone currently being studied include; non fossiliferous nature, absence of bioturbation, lack of stromatolite-like structure and ferruginous coatings as proposed by Ferretti (2005).

On the genetic model, previous researchers include Dymek and Klein (1988), Wonder *et al.* (1988), Derry and Jacobsen (1990) among others pointed out that patterns of element abundances preserved in ancient chemical sediments can be used to constrain the influence of seawater, hydrothermal, biogenic and detrital sources on the sediment composition. This study based the evaluation of origin of the ironstone in Share-Tsaragi area on differences in the mineralogical and chemical compositions. Texturally, color of the ironstone samples (yellowish-brown to reddish and dark brown) is illustrative of varying level of iron enrichment from iron pigmentation to partial and total iron replacement of the precursor materials. As presented in the petrographical and mineralogical data, dominance of goethite and hematite as iron phase might be the major driving mechanism for the formation of the ironstones formed during the long period of sub-aerial exposure and consequent oxidation. As submitted by Frost *et al.* (2003), the hematite which forms usually by dehydration of goethite through the removal of hydroxyl sheets, is very stable in an oxidizing environment but become unstable under reducing condition due to reduction from Fe^{3+} to Fe^{2+} . The goethite which is also present is a stable mineral at ambient temperature occur as a replacement of kaolinite and cement in the host sandstones. According to Lottermoser and Ashley (2000), element distribution and their abundance as preserved in sediments can be used to unravel the influence of terrestrial, hydrothermal, biogenic and detrital sources on the ironstone genesis. Dominance of iron mineral (hematite and goethite) assemblage, from the mineralogical result, suggest precipitation of oxyhydroxides that is likely to have been replaced by hematite through dehydration. The Paragenetic sequence and diagenetic history model (Fig. 10a) and proposed genetic model for the ironstone in this (Fig. 10b) also supported the ironstone formation during diagenesis. Based on the available geochemical data in this present work, there is similarity in the concentration of TiO_2 and Al_2O_3 with the Garra and Hussainiyat sedimentary ironstones as reported by Tobia (1983) and the iron rich beds reported by Babalola *et al.* (2003).

Comparison with Some Selected Sedimentary Ironstones

In an attempt to understand regional significance of the present study and further characterize and genesis of the investigated ironstones, a discussion on the comparison with the published data of known sedimentary ironstones is presented here. Data from Agbaja, Batati and Patti ironstones in the Bida Basin, Nigeria, Leru ironstone from Anambra Basin, Nigeria, Weald Basin ironstone from England and Bahariya ironstone from Egypt were adopted. Parameters considered are essentially the age, texture and structure, mineralogy, elemental composition and origin (see Table 5). Texturally, the present study belongs to Maastrichtian in age and thus equivalent laterally to the ironstones from Agbaja, Batati and Patti in the Bida Basin. Though, Agbaja and Batati ironstones are oolitic and pisolitic, meanwhile, Share-Tsaragi ironstones are best described as massive, lacking any internal structure. Further consideration of the mode of occurrence and lithological characteristics also show that the Patti ironstones and the Lower Cretaceous Weald basin, Cenomanian Bahariya occur as a lenticular bed and rhythmically bedded with sandstones and argillaceous rocks in some cases, whereas, the investigated ironstone is massively bedded and occur as a resistant cap over the sandstones and claystones. It also important to note that the according to Ojo *et al.* (2020) and Akande and Mucke (1993), the Maastrichtian Patti Formation ironstone exposed at Ahoko, southern Bida Basin and the Leru ironstones in Anambra Basin respectively are bioclastic, the Share-Tsaragi ironstones are non-fossiliferous like the Agbaja ironstones.

There is marked difference in the mineral and elemental compositions of the ironstones from Share-Tsaragi area compared to Weald, Bahariya, Patti and Leru (Table 5). The ironstones from Leru (Anambra basin) is not only sideritic but chamositic (Akande and Mucke 1993) whereas Bahariya ironstones, as reported by Afify *et al.* (2015) is composed of minor siderite with Fe-dolomite, ankerite, goethite and hematite as the main iron-bearing minerals. Significantly, the ironstones from Share-Tsaragi area contain mainly goethite and hematite with no siderite contents, whereas, the compared data have low to high amounts of siderite. The geochemical data of the present study reveal significantly lower concentration of Fe_2O_3 and higher SiO_2 with Al_2O_3 in contrast to Agbaja, Weald basin and Bahriya. Also, MgO and CaO is lower in the studied Share-Tsaragi ironstones when compared with the other referenced ironstones in this study. According to Akinlotan (2019),

the Weald basin ironstones were formed in a very low salinity to fresh water condition while Leru Ironstone and Patti Formation ironstones at Ahoko were interpreted by Ojo *et al.* (2020) and Mücke (2000) respectively to have been formed in more full saline water. Also, Mücke (2000) submitted that ooidal structures of the Agbaja Ironstone were mechanically formed through reworking processes caused by high energy tidal waves in a marginal environment. The mechanism of ferruginization related to the migration of iron rich fluids through pathways provided by permeable bedding planes and vertical fractures and consequent precipitation under anoxic condition and active roles of meteoric water and sea water as proposed for Bahariya by Afify *et al.* (2018) and Patti ironstones by Ojo *et al.* (2020) is ruled out in the Share-Tsaragi ironstones. Therefore, the ironstone from Share-Tsaragi area is interpreted to have sourced from diagenetic alteration and laterization of the precursor sandstone in oxidizing continental setting.

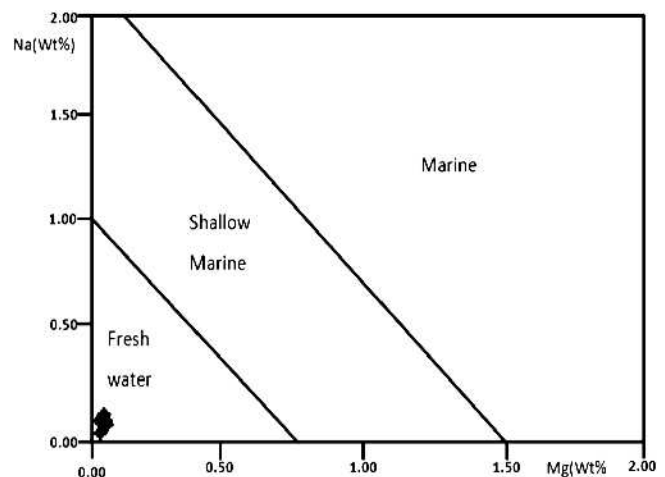


Fig. 8: Binary plot of Na against Mg after Nicholson (1992). Note all the studied samples plotted within the fresh water field.

Conclusions

The ironstones in Share-Tsaragi area of the northern Bida Basin are generally clayey and sandy and they are dominated by goethite and hematite. Quartz and kaolinite represent the original detrital precursors of the ironstones.

Encrustation and cementation of the poorly sorted quartz rich sandstones with iron minerals under oxidizing condition were the main driving processes in the formation of the investigated ironstones. The sandstones and claystones bearing the iron minerals in this area are interpreted to be sourced from the intensely weathered Basement Complex rocks from adjoining areas. The ironstones were formed by the deposition of

Table 5: Comparison of the studied ironstone with other ironstones from some selected locations.

Features		Locations						
		<i>Share-Tsaragi ironstone, Northern Bida Basin (Present Study)</i>	<i>Patti ironstone, Southern Bida Basin (Ojo et al., 2020)</i>	<i>Agbaja ironstone Southern Bida Basin (Mucke, 2000)</i>	<i>Batati ironstone, Northern Bida Basin (Mucke, 2000)</i>	<i>Leru ironstone, Anambra Basin (Mucke, 2000)</i>	<i>Bahariya ironstone, Egypt (Afify et al., 2018)</i>	<i>Weald Basin ironstone, England (Akinlotan, 2019)</i>
Age		Maastrichtian	Maastrichtian	Maastrichtian	Maastrichtian	Maastrichtian	Cenomanian (Host rock) and Coniacian to Turonian (Ironstone)	Lower Cretaceous
Texture/structure		Massive, poorly sorted, matrix rich, primary sandstone	Spheroidal, concretionary, massive, bioturbated and laminated, and fossiliferous and occur within shales	Thick oolitic to pisolitic	Oolitic/Pisolitic	Bioturbated and fossiliferous, oolitic, bands within Shales	Thin massive bands, concretions within siliciclastic rocks	Nodular, tabular and spherulitic, interbedded with mudstones and sandstones
Mineralogy		Goethite, Hematite, Kaolinite and quartz	Siderite, magnesian siderite, kaolinite and haematite	Kaolinite type, goethite and apatite	Kaolinite, goethite and haematite	Siderite, Chamosite type	Goethite, hematite, dolomite, ankerite and minor siderite	Siderite, illite and kaolinite
Major Elements (%)	SiO ₂	9.56-55.05	8.41-52.50	2.65-45.57	1.83-45.60	-	2.95-5.84	-
	Al ₂ O ₃	3.15-15.13	1.79-7.49	5.01-38.43	2.09-38.80	-	0.19-0.88	-
	CaO	0.01-0.08	1.41-13.97	Absent to low	0.00 - 0.22	-	≤ 12	0.30-2.30
	MgO	0.04-0.11	0.05-2.84	0.00-0.40	-	0.50-6.75	≤ 8.50	0
	Fe ₂ O ₃	26.01-77.62	36.46-49.72	-	-	-	-	-
Driving Mechanism		Ferruginization and laterization through meteoric water.	Active roles of meteoric water and sea water. Fractures and bedding planes as migration pathways	Ferruginization through meteoric water.	Ferruginization through meteoric water.	Influence of seawater	Influence of meteoric water enhanced by organic matter decomposition and HC migration. Fractures and permeable rock as conduits	Active roles of meteoric water and bacterial activities. Discontinuities as migration pathways for fluids.
Origin		Post-depositional, diagenetic modification under oxidizing and fresh water conditions	Post-depositional, diagenetic modification under anoxic and freshwater - full marine conditions	Replacement of kaolinite by goethite in low salinity water	Replacement of kaolinite by goethite in low salinity water	Fully Marine Condition	Diagenetic origin. Replacement of host by iron bearing minerals	Part depositional diagenetic modification. freshwater anoxic conditions

iron oxy-hydroxide as clay replacement and chemical precipitates of goethite and hematite within pores of stream laid detrital quartz grains and clays.

The study concludes that laterization process was involved in the formation of the ironstones. As indicated in our genetic model, the host sandstones were deposited in fluvial environments. No evidence of marine reworking and therefore it is different from the well known Agbaja Ironstone in the southern Bida Basin

and Leru Anambra Basin, Nigeria. The chemical composition of the ironstones is very similar to well-known sedimentary ironstones from around the world that are of diagenetic supergene enrichment and replacement of detrital precursor.

Acknowledgements

The authors appreciate the support from Tetfund National Research Fund Batch 2020 grant to the first

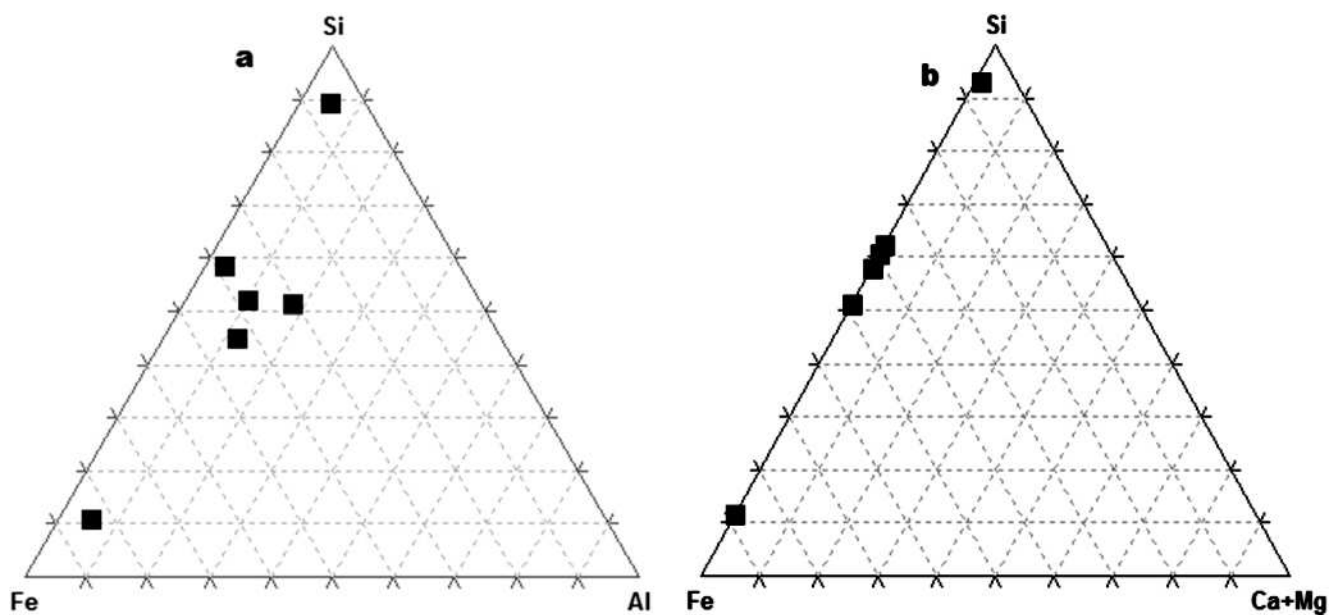


Fig. 9: Ternary plots of (a) Si-Fe-Al and, (b) Si-Fe-(Ca+Mg) for the Share-Tsaragi ironstones. Note that the two plots after Lottermoser and Ashley (2000) confirm the sedimentary origin of the studied ironstones.

Process	a	Depositional	Diagenesis		
			Early	Middle	Late
Detrital quartz and other precursor materials derived from weathering		█			
Formation of clay minerals (mainly Kaolinite)		█			
Precipitation of goethite cement			█		
Replacement of goethite by hematite				█	

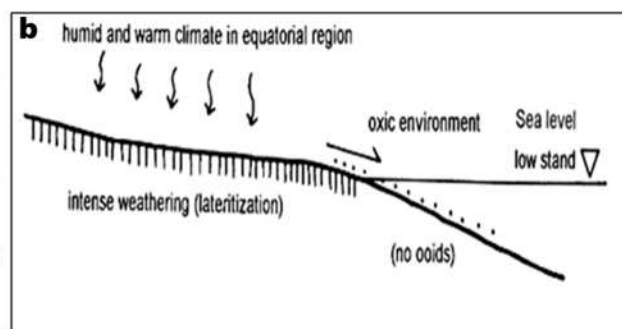


Fig. 10: (a) Paragenetic sequence and diagenetic history model of the investigated ironstones and (b) Genetic model for the formation of the Share-Tsaragi ironstone (Adapted from Yoshida et al., 1998).

author and the Management of the Federal University Oye-Ekiti, for the fieldwork support. The reviewers are

also appreciated for their suggestions.

References

Abimbola, A.F., Badejoko, T.A., Elueze, A.A. and Akande, S.O. (1999). The Agbaja ironstone formation, Nupe basin, Nigeria: A product of replacement of a kaolinite precursor. *Global Journal of Pure Applied Sciences*, 5, 375–384.

Adegoke, A.K., Abdullah, W.H., Hakimi, M.H. and Yandoka, B.M.S. (2014). Organic and inorganic geochemical characterization of Fika Formation in the Chad (Bornu) Basin. Northeastern Nigeria Implications for Depositional Environments and Tectonic Setting. *Applied Geochemistry*, 43, 1–12.

- Adeleye, D.R. (1973). Origin of ironstones, an example from middle Niger valley. *Journal of Sedimentary Petrology*, 43, 709–727.
- Adeleye, D.R. (1989). The Geology of the Middle Niger Basin: In: *Geology of Nigeria*, Kogbe, C.A. (ed.), *Geology of Nigeria (2nd edition)*, Elizabethan Publication Company, Lagos, 283–287.
- Adepoju, S.A., Ojo, O.J., Akande, S.O. and Sreenivas, B. (2021). Petrographic and geochemical constraints on petrofacies, provenance and tectonic setting of the upper Cretaceous sandstones, Northern Bida Basin, north-central Nigeria. *Journal of African Earth Sciences*, 174, 104041.
- Afify, A.M., Sanz-Montero, M.E., Calvo, J.P. and Wanas, H.A. (2015). Diagenetic origin of ironstone crusts in the lower cenomanian Bahariya formation, Bahariya depression, western desert Egypt. *Journal of African Earth Sciences*, 101, 333–349.
- Afify, A.M., Sanz-Montero, M.E., Calvo, J.P. (2018). Differentiation of ironstone types by using rare earth elements and yttrium geochemistry: A case study from the Bahariya region, Egypt. *Ore Geology Review*, 96, 247–261.
- Akande, S.O. and Mucke, A. (1993). Depositional Environments and diagenesis of carbonates at the Mamu/Nkporo Formation transition, Anambra Basin, southern Nigeria. *Journal of African Earth Sciences*, 17, 445–456.
- Akande, S.O., Ojo, O.J., Erdtmann, B.D. and Hetenyi, M. (2005). Paleoenvironments, Organic petrology and Rock-Eval studies on source rock facies of the lower Maastrichtian Patti Formation, Southern Bida Basin, Nigeria. *Journal of African Earth Sciences*, 41, 394–406.
- Akinlotan, O. (2019). Sideritic ironstones as indicators of depositional environments in the Weald Basin (Early Cretaceous), SE England. *Geological Magazine*, 156, 533–546.
- Babalola, L.O., Hussain, M. and Hariri, M.M. (2003). Origin of iron-rich beds in the basal Wajid sandstone, Abha-Khamis Mushayt area, Southwest Saudi Arabia. *Arabian Journal for Science Engineering*, 28, 3–24.
- Barwise, A.J.G. (1990). Role of nickel and vanadium in petroleum classification. *Energy and Fuels*, 4, 647–652.
- Boyd, T. and Scott, S.D. (1999). Two-XRD-line ferrihydrite and Fe–Si–Mn oxyhydroxide mineralization from Franklin Seamount, western Woodlark Basin, Papua New Guinea. *The Canadian Mineralogy*, 37, 973–990.
- Braide, S.P. (1992). Syntectonic Fluvial Sedimentation in the Central Bida Basin. *Journal of Mining and Geology*, 28, 55–64.
- Clarke, J.D.A. and Chenoweth, L. (1996). Classification, genesis and evolution of ferruginous surface grains. *Journal of Australian Geology and Geophysics*, 16, 213–221.
- Cornell, R.M. and Schwertmann, U. (2003). *The iron oxides: structure, properties, reactions, occurrences and uses (2nd Edition)*. Wiley - VCH, Weinheim, 664 p.
- Cotter, E. and Link, J.E. (1994). "Deposition and Diagenesis of Clinton Ironstones (Silurian) in the Appalachian Foreland Basin of Pennsylvania". *Geological Society of America Bulletin*, 105, 911–922.
- Deng, H.W. and Qian, K. (1993). *Analysis on Sedimentary Geochemistry and Environment*. Science Technology Press, Gansu, 85 p. (in Chinese)
- Ferretti, A. (2005). Ooidal ironstones and laminated ferruginous deposits from the Silurian of the Carnic Alps. *Austria Bollettino della Società Paleontologica Italiana*, 44, 263–278.
- Frost, R.L., Ding, Z. and Ruan, H. (2003). Thermal analysis of goethite, Relevance to Australian indigenous art. *Journal of Thermal Analysis and Calorimetry*, 71, 783–797.
- Fu, X., Wang, J., Zeng, Y., Cheng, J. and Tano, F. (2011). Origin and mode of occurrence of trace elements in marine oil shale from the Shengli River area, Northern Tibet, China. *Oil Shale*, 28, 487–506.
- Gloaguen, E., Branquet, Y., Boulvais, P., Moelo, Y., Chauvel, J.J. and Chiappero, P.J. (2007). Palaeozoic oolitic ironstone of the French Armorican Massif: A chemical and structural trap for orogenic base metal–As–Sb–Au mineralization during Hercynian strike-slip deformation. *Mineralium Deposita*, 42, 399–422.
- Gutzmer, J., Chisonga, B.C., Beukes, N.J. and Mukhopadhyay, J. (2008). The Geochemistry of Banded Iron Formation-Hosted High-Grade Hematite-Martite Iron Ores. *Society of Economic Geology (SEG Review)*, 15, 157–183.
- Hatch, J.R. and Leventhal, J.S. (1992). Relationship between inferred redox potential of the depositional environment and geochemistry of the Upper Pennsylvanian (Missourian) stark shale member of the Dennis Limestone, Wabaunsee County, Kansas, USA. *Chemical Geology*, 99, 65–82.

- Hein, J.R., Schulz, M.S., Dunham, R.E., Stern, R.J. and Bloomer, S.H. (2008). Diffuse flow hydrothermal manganese mineralization along the active Mariana and southern IzuBonin arc system, western Pacific. *Journal of Geophysical Research*, 113, 1–29.
- James, H.L. (1966). Chemistry of the iron-rich sedimentary rocks. U.S. Geological Survey Professional Paper, 440W, 47–60.
- Jones, B. and Manning, D.A.C. (1994). Comparison of geochemical indices used for the interpretation of palaeoredox conditions in ancient mudstones. *Chemical Geology*, 111, 111–129.
- Kennedy, W.Q. (1965). The influence of basement structure on the evolution of the coastal (Mesozoic and Tertiary) basins. In: *Recent Basins around Africa*. Proceeding of Institute of Petroleum Geological Society of London, 35–47.
- Khan, R.M.K., Sharma, S.D., Patil, D.J. and Naqvi, S.M. (1996). Trace, rare-earth element, and oxygen isotopic systematics for the genesis of banded iron-formations: Evidence from Kushtagi schist belt, Archean Dharwar Craton, India. *Geochimica et Cosmochimica Acta*, 60, 3285–3294.
- King, L.C. (1950). Outline and distribution of Gondwanaland. *Geological Magazine*, 87, 353–359.
- Kogbe, C.A., Ajakaiye, D.E., Matheis, G., 1983. Confirmation of Rift Structure along the Mid-Niger Valley, Nigeria. *Journal African Earth Sciences*, 1, 127–131.
- Ladipo, K.O., Akande, S.O. and Mücke, A. (1994). Genesis of Ironstones from the Middle Niger Sedimentary Basin, Evidence from Ore Microscopic and Geochemical Studies. *Journal of Mining and Geology*, 30, 161–168.
- Lepp, H. and Goldich, S.S. (1964). "Origin of Precambrian Iron Formation". *Economic Geology*, 58, 1025–1061.
- Lewan, M.D. (1984). Factors controlling the proportionality of vanadium to nickel in crude oils. *Geochimica et Cosmochimica Acta*, 48, 2231–2238.
- Liu, B.J. (1980). Sedimentary petrology. Geological Press, Beijing, 89 p. (in Chinese)
- Loope, D.B., Kettler, R.M. and Webber, K.A. (2012). Morphologic clues to the origins of iron oxide-cemented spheroids, boxworks, and pipelike concretions, Navajo Sandstone of South-Central Utah, U.S.A. *Journal of Geology*, 119, 505–520.
- Lottermoser, B.G. and Ashley, P.M. (1996). Geochemistry and exploration significance of ironstones and barite-rich rocks in the Proterozoic Willyama Supergroup, Olary Block, South Australia. *Journal of Geochemical Exploration*, 57, 57–73.
- Lottermoser, B.G. and Ashley, P.M. (2000). Geochemistry, petrology and origin of Neoproterozoic ironstones in the eastern part of the Adelaide Geosyncline, South Australia. *Precambrian Research*, 101, 49–67.
- MacDonald, R., Hardman, D., Sprague, R., Meridji, Y., Mudjiono, W., Galford, J., Rourke, M., Dix, M. and Kelto, M. (2010). Using elemental geochemistry to improve sandstone reservoir characterization: a case study from the Unayzah A interval of Saudi Arabia. *Society of Petrophysicists and Well Log Analyst 51st Annual Logging Symposium*, Jun. 19–23, p. 1–16.
- Monaco, S.L., Lopez, L., Rojas, H., Garcia, D., Premovic, P. and Briceno, H. (2002). Distribution of major and trace elements in La Luna Formation, Southwestern Venezuelan Basin. *Organic Geochemistry*, 33, 1593–1608.
- Mücke, A. (2000). Environmental conditions in the late Cretaceous African Tethys: conclusions from a microscopic-microchemical study of ooidal ironstones from Egypt, Sudan and Nigeria. *Journal of African Earth Sciences*, 30, 25–46.
- Mücke, A., Badejoko, T.A. and Akande, S.O. (1999). Petrographic, mechanical studies and origin of Agbaja Phanerozoic ironstone formation, Nupe Basin, Nigeria: a product of ferruginised ooidal kaolin precursor not identical to the Minette type. *Mineralium Deposita*, 34, 284–296.
- Nicholson, K. (1992). Genetic types of manganese oxide-deposits in Scotland: Indicators of Paleoocean spreading rate and a Devonian Geothermal mobility boundary. *Economic Geology*, 87, 1301–1309.
- Ojo, O.J. (2012). Depositional Environments and Petrographic Characteristics of Bida Formation around Share-Pategi, Northern Bida Basin, Nigeria. *Journal of Geography and Geology*, 4, 224–241.
- Ojo, O.J. and Akande, S.O. (2012). Sedimentary facies relationships and depositional environments of the Maastrichtian Enagi Formation, Northern Bida Basin, Nigeria. *Journal of Geography and Geology*, 4, 136–147.
-

- Ojo, O.J., Bamidele, T.E., Adepoju, S.A. and Akande, S.O. (2020). Genesis and paleoenvironmental analysis of the ironstone facies of the Maastrichtian Patti Formation, Bida Basin, Nigeria. *Journal of African Earth Sciences*, 174, 104058.
- Ojo, S.B. and Ajakaiye, D.E. (1989). Preliminary interpretation of gravity measurements in the middle Niger Basin area, Nigeria: In: Kogbe, C.A. (Editor), *Geology of Nigeria* (2nd edition) Elizabethan Publishing Company, Lagos, 347–358.
- Olaniyan, O. and Olobaniyi, S.B. (1995). Facies analysis of the Bida sandstone formation around Kajita, Nupe basin, Nigeria. *Journal of African Earth Sciences*, 23, 253–255.
- Olugbemiro, R. and Nwajide, C.S. (1997). Grain Size Distribution and Particle Morphogenesis as Signatures of Depositional Environment of Cretaceous (non-Ferruginous) Facies in the Bida Basin, Nigeria. *Journal of Mining and Geology*, 33, 89–101.
- Salama, W., El Aref, M. and Gaupp, R. (2012). Mineralogical and geochemical investigations of the Middle Eocene ironstones, El Bahariya Depression, Western Desert, Egypt. *Gondwana Research*, 22, 717–736.
- Tobia, F.H. (1983). Geochemistry and mineralogy of the iron ore deposits of Gaara formation in Iraqi western desert. Master Thesis, Baghdad University, 156 p.
- Tucker, M.E. (1981). *Sedimentary petrology, an introduction*. Blackwell Scientific Publications, Oxford, 252 p.
- Udensi, E.E., Osazuwa, I.B. (2004). Spectra determination of depths to Magnetic rocks under the Nupe basin, Nigeria. *Nigerian Association of Petroleum Explorationists Bulletin*, 17, 22–37.
- Wang, A.H. (1996). Discriminant defect of sedimentary environment by the Sr/Ba ratio of different existing forms. *Acta Sedimentologica Sinica*, 14, 168–173.
- Yoshida, M., Khan, I.H. and Ahmad, M.N. (1998). Remanent magnetization of oolitic ironstone beds, Hazara area, Lesser Himalayan thrust zone, Northern Pakistan: Its acquisition, timing, and paleoenvironmental implications. *Earth Planet Space*, 50, 733–744.
- Young, T.P. and Taylor, W.G.E. (1989). *Phanerozoic ironstones*. Geological Society of London Special Publication, 46, 251 p.
-